

# Preparation and Solid-State Properties of Self-Assembled Dinuclear Platinum(II) and Palladium(II) Rhomboids from Carbon and Silicon Tectons

Marion Schmitz, Stefan Leininger, Jun Fan, Atta M. Arif, and Peter J. Stang\*

Department of Chemistry, University of Utah, Salt Lake City, Utah 84112

Received July 19, 1999

Self-assembly reactions of hitherto unknown bis(4-pyridyl)silanes **2a,b** with bis(triethylphosphine)platinum and bis(triethylphosphine)palladium bistriflates **5a,b** lead to the formation of new silicon-containing rhomboids **6a–d**. In addition, a similar carbon analogue **7** was prepared by reaction of bispyridyl acetal **4** and bis(triethylphosphine)platinum bistriflate (**5a**). Surprisingly, reaction of the bis(4-pyridyl)ketone (**3**) and the platinum complex **5a** gave a similar rhomboid, **10**, due to unexpected hydration of the ketone. The crystal structures of silicon complex **6a** and its carbon analogue **7** were solved and compared to each other as well as to already known carbon-containing dinuclear rhomboids. In addition, the dinuclear bisporphyrin complex **8** was also characterized by X-ray structure analysis. Electrospray and FAB mass spectral data are reported as well, confirming the binuclear nature of the entities formed.

## Introduction

Self-assembly via dative bonding of bidentate nitrogen-containing ligands with transition metal complexes is a widely used methodology in supramolecular chemistry.<sup>1</sup> Such systems as helicates,<sup>2</sup> catenanes,<sup>3</sup> cylinders,<sup>4</sup> and other three-dimensional cage compounds<sup>5</sup> have been prepared. Much progress has been made in the design of molecules that can act as host molecules for organic guests,<sup>5,6</sup> and the physical basis of self-assembly macrocyclizations is the subject of current research.<sup>7</sup> Over the past few years, the synthesis of diverse molecular squares and rectangles has been reported,<sup>5,8</sup> but only a few publications show the design of parallelograms with other than 90° angles at the corners.<sup>9–11</sup> Our interest focused on the synthesis of new silicon-

containing pyridine-based linker units with tetrahedral angles of 109° and the self-assembly of hitherto unknown silicon-containing supramolecular parallelograms. The larger atomic size of silicon compared to carbon is especially important for the synthesis of cyclic compounds and possible host–guest chemistry within the cavities of these molecules.<sup>12</sup> Due to their different electronegativities, the chemical bonding properties of silicon and carbon are quite different.<sup>13</sup> For example, the heavier carbon homologues tend to form bond angles of about 90°, resulting in less strained four-membered-ring systems.<sup>14</sup> Furthermore, silicon is able to expand its valence shell and to produce penta- or even hexavalent species.<sup>15</sup> Recently, pentacoordinated silicon compounds were used to build silicon-containing tetra-anionic molecular squares.<sup>16</sup> In this paper, we report novel silicon-containing binuclear tetracationic rhomboids incorporating either platinum or palladium, as well as carbon analogues, and discuss their solid-state structures.

## Results and Discussion

**Synthesis of the Tetrahedral Building Units 2 and 4.** For our purposes, the 4-pyridyl-substituted silanes **2a,b**, with tetrahedral angles between the nitrogen atoms, are necessary. The synthesis of **2a,b**

(1) Reviews: (a) Lehn, J.-M.; Atwood, J. L.; Davies, J. E. D., MacNicol, D. D., Vögtle, F., Eds. *Comprehensive Supramolecular Chemistry*; Pergamon: Oxford, 1996; Vol. 9, Chapters 1–8. (b) Olenyuk, B.; Fechtenkötter, A.; Stang, P. J. *J. Chem. Soc., Dalton Trans.* **1998**, 1707. (c) Stang, P. J.; Olenyuk, B. *Acc. Chem. Res.* **1997**, *30*, 502–518. (d) Lehn, J.-M. *Supramolecular Chemistry: Concepts and Perspectives*; VCH: Weinheim, 1995. (e) Caulder, D. L.; Raymond, K. N. *J. Chem. Soc., Dalton Trans.* **1999**, 1185. (f) Beissel, T.; Powers, R. E.; Raymond, K. N. *Angew. Chem., Int. Ed. Engl.* **1996**, *35*, 1084.

(2) McMorran, D. A.; Steel, P. J. *Angew. Chem., Int. Ed.* **1998**, *37*, 3295.

(3) Fujita, M. *Acc. Chem. Res.* **1998**, *32*, 53.

(4) Baxter, P. N. W.; Lehn, J.-M.; Baum, G.; Fenske, D. *Chem. Eur. J.* **1999**, *5*, 102.

(5) Fujita, M. *Chem. Soc. Rev.* **1998**, *27*, 417.

(6) Ruttimann, S.; Bernadelli, G.; Williams, A. F. *Angew. Chem., Int. Ed. Engl.* **1993**, *32*, 392.

(7) Ercolani, G. *J. Phys. Chem. B* **1998**, *102*, 5699.

(8) (a) Jeong, K.-S.; Cho, Y. L.; Song, J. U.; Chang, H.-Y.; Choi, M.-G. *J. Am. Chem. Soc.* **1998**, *120*, 10982. (b) Constable, E. C.; Schofield, E. J. *Chem. Soc., Chem. Commun.* **1998**, 403. (c) Duhme, A.-K.; Davies, S. C.; Hughes, D. L. *Inorg. Chem.* **1998**, *37*, 5380. (d) Woessner, S. M.; Helms, J. B.; Shen, Y.; Sullivan, B. P. *Inorg. Chem.* **1998**, *37*, 5406. (e) Benkstein, K. D.; Hupp, J. T.; Stern, C. L. *Inorg. Chem.* **1998**, *37*, 5404. (f) Benkstein, K. D.; Hupp, J. T.; Stern, C. L. *J. Am. Chem. Soc.* **1998**, *120*, 12982.

(9) Fujita, M.; Aoyagi, M.; Ogura, K. *Inorg. Chim. Acta* **1996**, *246*, 53.

(10) Habicher, T.; Nierengarten, J.-F.; Gramlich, V.; Diederich, F. *Angew. Chem., Int. Ed. Engl.* **1998**, *37*, 1916.

(11) Hartshorn, C. M.; Steel, P. J. *Inorg. Chem.* **1996**, *35*, 6902.

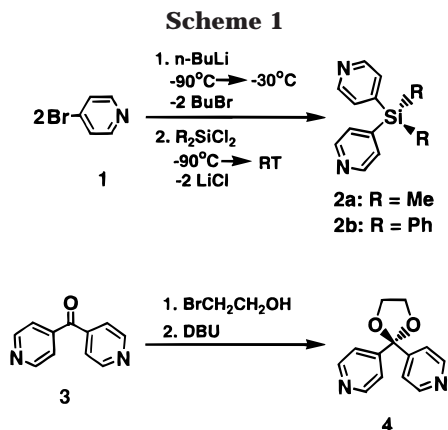
(12) Guo, L.; Hrabusa, J. M., III; Senskey, M. D.; McConville, D. B.; Tessier, C. A.; Youngs, W. J. *Organometallics* **1999**, *18*, 1767.

(13) Allred, A. L. *J. Inorg. Nucl. Chem.* **1961**, *17*, 215.

(14) Sekiguchi, A.; Nagase, S. *Chem. Org. Silicon Compd.* **1998**, *2*, 119.

(15) Jung, M. E.; Xia, H. *Tetrahedron Lett.* **1988**, *29*, 297.

(16) McCord, D. J.; Small, J. H.; Greaves, J.; Van, Q. N.; Shaka, A. J.; Fleischer, E. B.; Shea, K. J. *J. Am. Chem. Soc.* **1998**, *120*, 9763.

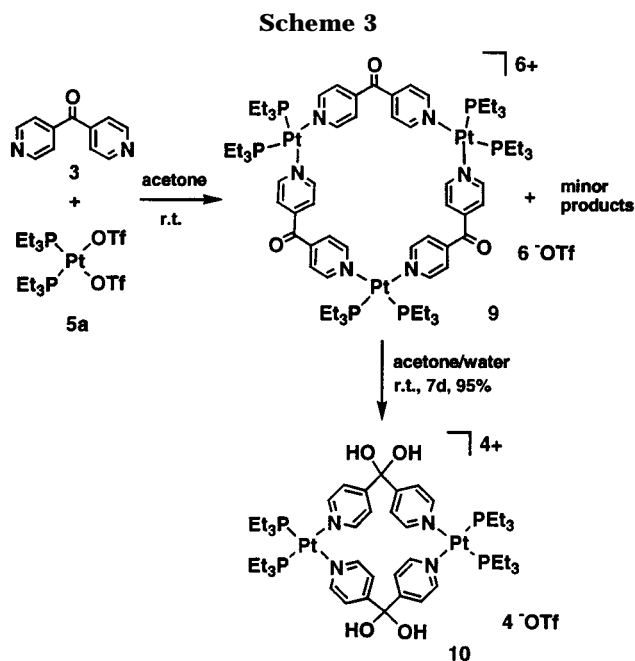
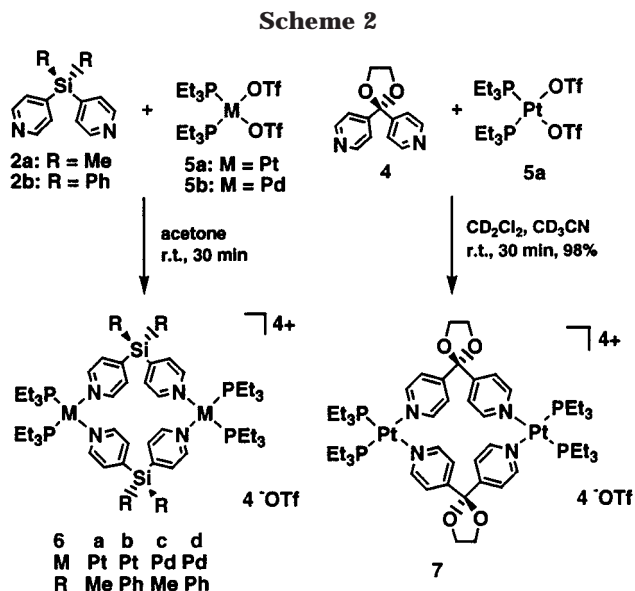


was achieved analogously to literature procedures<sup>17,18</sup> for the preparation of 2- and 3-pyridyl-substituted silanes from the corresponding bromide. 4-Bromopyridine (**1**) underwent lithium halogen exchange with *n*-butyllithium to give the corresponding pyridyllithium. Treatment of this reaction mixture with 0.5 equiv of dichlorosilane at  $-90^\circ\text{C}$  lead to the formation of the bispyridylsilanes **2** (Scheme 1). The dimethyl compound **2a** was obtained after workup as a yellow oil in 24% yield. The diphenyl analogue **2b** was obtained as white crystals (46% yield).

The analogous carbon building unit, bis(4-pyridyl)acetal **4**, was obtained by reaction of a toluene solution of bis(4-pyridyl)ketone (**3**) with 2-bromoethanol in the presence of DBU (Scheme 1).

The composition of the new building blocks **2** and **4** were confirmed by microanalytical and mass spectrometric data. The NMR data of **2** and **4** showed the expected patterns: the  $^{29}\text{Si}$  NMR spectra of **2** consisted of singlets around 0 to  $-10$  ppm, which were in the typical region for alkyl- and aryl-substituted silanes. The absorptions for the pyridyl protons in the  $^1\text{H}$  NMR spectra of **2** and **4** were found in the normal aromatic range, as were the phenyl protons in **2b**. The signal for the methyl protons in **2a** were close to 0 ppm, whereas the methylene protons in **4** resonated at 4.11 ppm. The integration of the proton NMR of **2** clearly showed the 1:1 ratio of pyridyl groups to methyl or phenyl substituents. The ketal structure of **4** was obvious in the  $^{13}\text{C}$  NMR, where the signal of the quaternary carbon atom surrounded by two oxygen atoms was found at 108.3 ppm. A single crystal of **2b** suitable for X-ray crystallography was obtained by crystallization from methylene chloride/diethyl ether at  $-20^\circ\text{C}$ . Crystals of the bis(4-pyridyl)silane **2b** were tetragonal, with space group *P421c*. Due to a disorder in the crystal, the para-nitrogen atoms could not be distinguished from the para-carbon atoms in the aromatic rings. The angles around the central silicon are nearly tetrahedral ( $110.02(5)^\circ$  and  $108.38(9)^\circ$ ), as expected.

**Formation of Rhomboids 6a–d and 7.** The bispyridyl compounds **2** and **4** can be used to self-assemble macrocycles via dative bonding of the pyridyl groups to the transition metal centers. The self-assembly of the silicon-containing rhomboids **6** proceeded in nearly quantitative yields by reaction of the bispyridyl silanes



**2** with the metal bistriflate complexes **5** in a 1:1 ratio in acetone (Scheme 2). To compare the silicon-containing rhomboids **6** to an analogous carbon species, the all-carbon rhomboid **7** was self-assembled in a similar manner (Scheme 2). Reaction of the tetrahedral building block **4** with the bistriflate complex **5a** in acetone gave the cyclic bisplatinum compound **7** in excellent yield. All five dinuclear complexes gave stable microcrystalline white or light yellow solids. They were fully characterized by analytical and spectral means as outlined in the Experimental Section. The spectral properties of rhomboid **7** are comparable to those of the rhomboids **6**.

The  $^{31}\text{P}\{^1\text{H}\}$  NMR spectra of each rhomboid showed a sharp singlet in the expected range. For the platinum complexes **6a,b** and **7**, the  $^{31}\text{P}$  signals were around 5 to 0 ppm with  $^1J(\text{Pt},\text{P})$  coupling constants between 3080 and 3070 Hz, and for the phosphorus atoms of the palladium systems **6c,d** these were at 32 and 36 ppm, respectively. The resonances were shifted upfield relative to the starting complexes **5a,b** due to ligation. The

(17) Wright, M. E. *Tetrahedron Lett.* **1987**, 28, 3233.

(18) Zeldin, M.; Xu, J.-M.; Tian, C.-X. *J. Organomet. Chem.* **1987**, 326, 341.

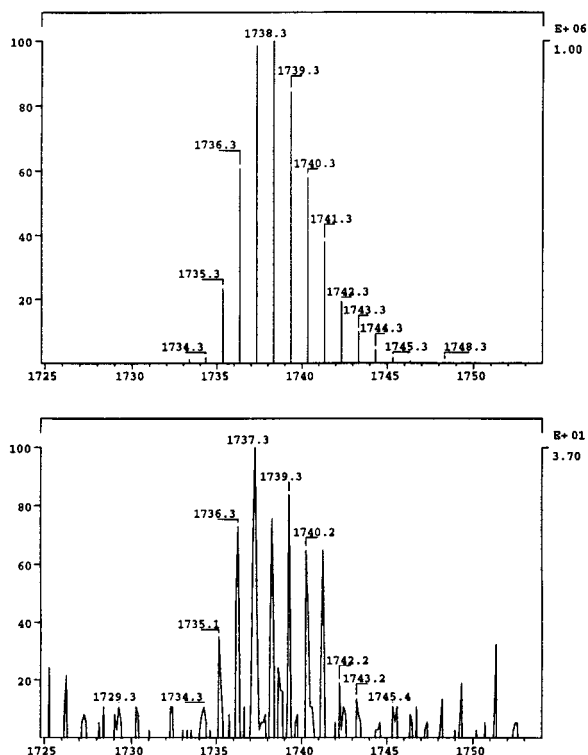


**Figure 1.** Calculated (top) and experimental (bottom) isotopic distribution pattern of M-OTf for **6a** (FABMS).

$^{29}\text{Si}$  NMR spectra of **6a–d** displayed singlets at 0 ppm for the methyl compounds **6a,c** and at  $-10$  ppm for the phenyl-substituted products **6b,d**, with only a small shift relative to the starting materials **2**. Diagnostic for the dinuclear rhomboids **6** and **7** were the respective  $^1\text{H}$  and  $^{13}\text{C}\{^1\text{H}\}$  NMR spectra. The  $^1\text{H}$  NMR signals for the  $\beta$ -pyridyl protons were shifted downfield, relative to the precursors **2** and **4**, while the signals for the  $\alpha$ -pyridyl protons remained essentially unchanged. This low-field shift was due to the dative bonding of the nitrogen lone pair to the transition metal, as expected. Integration of the proton signals was in accord with the requirements for **6a–d** and **7**. The methyl carbon atoms of the Si-CH<sub>3</sub> group in **6a,c** were detected at  $-5.7$  ppm in the  $^{13}\text{C}$  NMR with a small high-field shift relative to **2a**.

Fast atom bombardment mass spectrometric (FABMS) analysis of cyclophanes **6a,b,d** gave a M-OTf peak at 1738 amu (**6a**), 1987 amu (**6b**), and 1809 amu (**6d**), each with a +1 charge state (separation of peaks by 1.0  $m/z$ ). The isotopic distribution patterns were within experimental error of the respective calculated compositions of these species. The calculated and experimental M-OTf signal for rhomboid **6a** is shown in Figure 1. Electrospray mass spectra of **6** and **7** showed different results depending on the substitution pattern on the silicon and the organic linker units. For the methyl-containing products **6a,c** the M-OTf peaks at 1738 amu (**4a**) and 1560 amu (**4c**) were observed. The +1 species of the phenyl compounds **6b,d** and rhomboid **7** were not stable enough under the conditions, and fragmentation occurred. In all three spectra the M/2-OTf species were detected.

In addition, rhomboids **6a** and **7** were examined by single-crystal X-ray diffraction, thus unambiguously establishing the structures of these novel silicon- and

carbon-containing self-assembled dinuclear rhomboids, both in the solid state (X-ray) and in solution (FABMS and ESMS).

#### Molecular Structure of Rhomboids **6a**, **7**, and **8**.

An X-ray crystallographic study for each of the three compounds **6a**, **7**, and **8** was carried out. Crystal data for these complexes are given in Table 1. Crystals of **6a** and **7** suitable for X-ray structure analysis were obtained by slow evaporation of an acetone solution, while crystals of the previously reported **8**<sup>19</sup> were obtained from chloroform.

The structure of the platinum–silicon complex **6a** is a parallelogram (Figure 2). The platinum(II) coordination is square planar with a significant deviation from the ideal 90° angles. While the N–Pt–N angle is 81.71(16)°, the corresponding P–Pt–N angles are opened up to 97.87(5)°. The inner dihedral angle at the quaternary silicon atom (Py–Si–Py) is 109°, close to tetrahedral and identical to the angle found for the precursor bisphenylbis(4-pyridyl)silane **2b**. The sum of the inner angles of the macrocyclic rhomboid is 381.0°, slightly larger than the 360° needed for a planar macrocycle. As a result of this increased sum of the angles, the pyridyl rings are bent outward in order to compensate for the higher ring strain. The core of this assembly, encompassing the two Pt centers, the silicon atoms, and the pyridyl N and C<sub>7</sub> atoms, deviates only slightly from the best plane. In addition, the pyridyl rings are twisted out of the rhomboidal plane, with angles of 72.61° and 78.11°. As a result of the crystallographic inversion center, the pyridyl rings of one bispyridyl silane unit are bent inward, whereas the pyridyl rings of the second bispyridyl silane unit are bent outward, resulting in parallel sets of opposing pyridyl rings. The two triethylphosphine ligands are twisted out of the rhomboidal plane by ca. 6° in accordance with the bending of the pyridyl rings. The Pt–P (2.27(1) Å) and the Pt–N (2.10(1) Å) bond lengths are within the standard range.<sup>20,21</sup> For the cavity, a diagonal Pt–Pt distance of 10.9 Å and a diagonal Si–Si distance of 8.0 Å is observed. Two triflate counterions were found and refined per asymmetric unit. They are located directly above and below the P<sub>2</sub>PtN<sub>2</sub> plane, with Pt–O distances of 3.45 and 3.60 Å, respectively. In addition, two acetone solvent molecules per asymmetric unit were found and refined. They are located outside the stacked parallelograms, filling up void space between the stacks. The stacked self-assembled systems are not perpendicular with respect to the stacking axis, but are tilted by an angle of roughly 42° (Figure 3). The shortest intermolecular stacking distance is 10.47 Å. This is similar to the stacking distance found for the neutral-charged mixed transition metal square<sup>20</sup> (10.7 Å) and for the hybrid iodonium–transition metal square (9.5 Å).<sup>21</sup>

The X-ray crystal structure of the carbon analogue **7** also shows a rhomboidal system with an N–Pt–N angle of 81.98(8)° and a tetrahedral angle of 110.1(4)° for the quaternary acetal carbon atom C1 (Figure 4). Least-

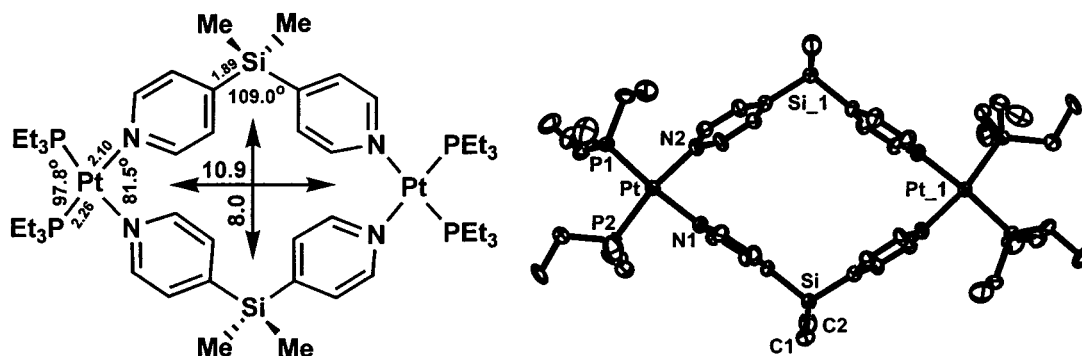
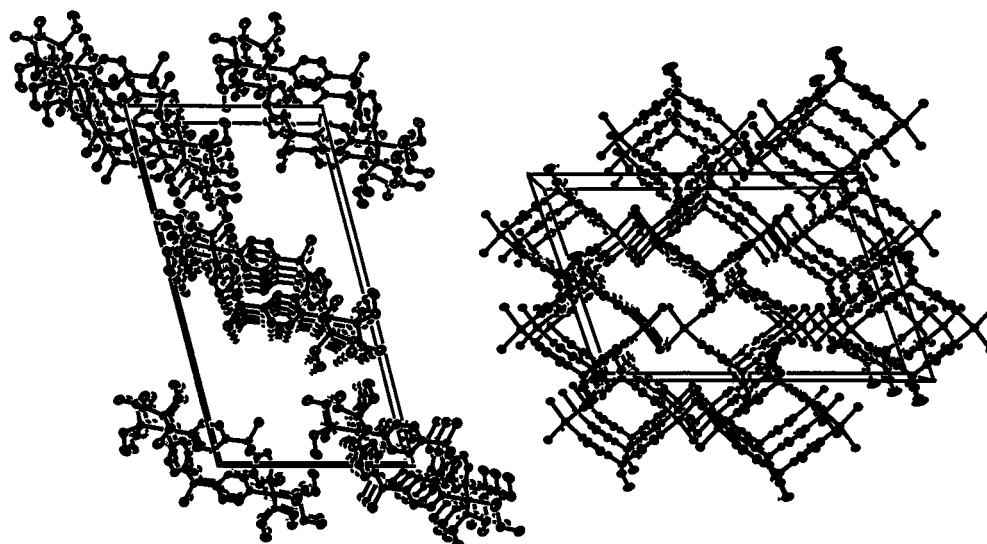
(19) Fan, J.; Whiteford, J. A.; Olenyuk, B.; Levin, M. D.; Stang, P. J.; Fleischer, E. B. *J. Am. Chem. Soc.* **1999**, *121*, 2741.

(20) Whiteford, J. A.; Lu, C. V.; Stang, P. J. *J. Am. Chem. Soc.* **1997**, *119*, 2524.

(21) Stang, P. J.; Chen, K.; Arif, A. M. *J. Am. Chem. Soc.* **1995**, *117*, 8793.

**Table 1. Crystallographic Data for the X-ray Diffraction Analysis of 6a, 7, and 8**

	6a	7	8
formula	C <sub>64</sub> H <sub>112</sub> F <sub>12</sub> N <sub>4</sub> O <sub>16</sub> P <sub>4</sub> Pt <sub>2</sub> S <sub>4</sub> Si <sub>2</sub>	C <sub>54</sub> H <sub>84</sub> F <sub>12</sub> N <sub>4</sub> O <sub>16</sub> P <sub>4</sub> Pt <sub>2</sub> S <sub>4</sub>	C <sub>156</sub> H <sub>154</sub> F <sub>12</sub> N <sub>12</sub> O <sub>21</sub> P <sub>4</sub> Pd <sub>2</sub> S <sub>4</sub>
fw (g)	2120.06	1915.55	3225.83
cryst syst	monoclinic	monoclinic	monoclinic
space group	<i>P2<sub>1</sub>/n</i>	<i>C2/c</i>	<i>P2<sub>1</sub>/n</i>
<i>a</i> (Å)	15.2277(6)	27.0947(6)	20.6530(5)
<i>b</i> (Å)	10.4690(2)	18.3342(4)	24.2278(3)
<i>c</i> (Å)	29.0020(10)	17.6983(4)	31.4736(7)
$\alpha$ (deg)	104.4380(11)	109.068(1)	101.8708(7)
<i>V</i> (Å <sup>3</sup> )	4477.4(2)	8309.4(3)	15411.8(5)
<i>Z</i>	2	4	4
<i>D</i> <sub>calcd</sub> (g cm <sup>-3</sup> )	1.573	1.531	1.390
$\lambda$ (Mo K $\alpha$ )	0.71073	0.71073	0.71073
<i>F</i> (000)	2136	3808	6664
$\mu$ (mm <sup>-1</sup> )	3.395	3.623	0.413
cryst size	0.28 × 0.10 × 0.03	0.30 × 0.30 × 0.25	0.20 × 0.15 × 0.15
$\theta$ range (deg)	2.92–20.62	2.56–30.05	2.13–26.32
<i>hkl</i>	+15,+10, $\pm$ 28	+38,+25, $\pm$ 24	+25,+27, $\pm$ 39
no. of total rflns	4131	12011	17794
no. of data ( <i>I</i> > 2 $\sigma$ ( <i>I</i> ))	3871	10118	17596
no. of params refined	487	608	1806
R1 ( <i>I</i> > 2 $\sigma$ ( <i>I</i> ))	0.0258	0.0530	0.0644
wR2 ( <i>I</i> > 2 $\sigma$ ( <i>I</i> ))	0.0612	0.1128	0.1816
GoF ( <i>I</i> > 2 $\sigma$ ( <i>I</i> ))	1.058	1.119	1.131
diff peak and hole (e Å <sup>-3</sup> )	–0.538 to 0.579	–0.926 to 1.484	–1.217 to 1.085

**Figure 2.** ORTEP plot representation and summary of the significant geometric features of the cationic portion of molecular rhomboid **6a**.**Figure 3.** Stacking diagram of the cationic portion of rhomboid **6a** (left) and **7** (right).

squares calculations show that the two Pt atoms and the quaternary carbon atom deviate by only 0.17 Å from the best plane. One set of parallel pyridyl rings is orthogonal with respect to this plane (89.5°), whereas the other set of parallel pyridyl rings are tilted by 70.8°. The P–Pt (2.28(1) Å) and the N–Pt (2.11(1) Å) bond

lengths are in the expected range. The cavity of this carbon analogue is slightly smaller than the cavity of **6a**, with a diagonal Pt–Pt distance of 10.2 Å and a diagonal C(quat)–C(quat) distance of 7.7 Å. Considering the van der Waals radii of platinum (~1.75 Å) and carbon (~0.8 Å), the effective Pt–Pt distance shrinks

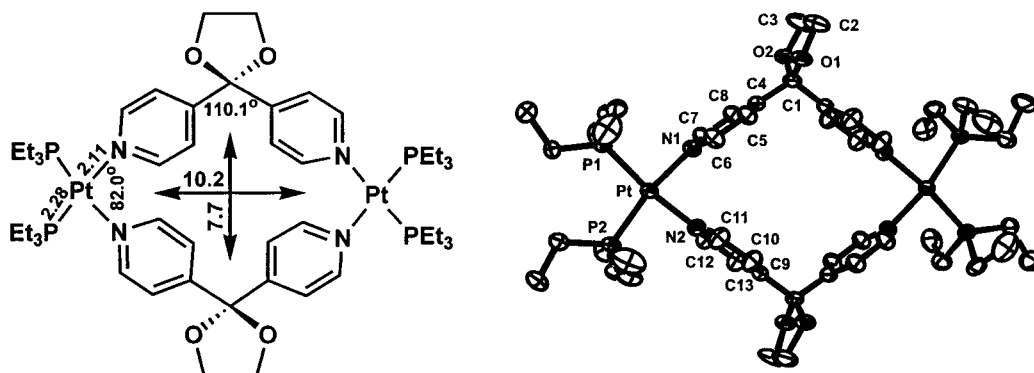


**Figure 4.** ORTEP plot representation and summary of the significant features of molecular rhomboid **7**.

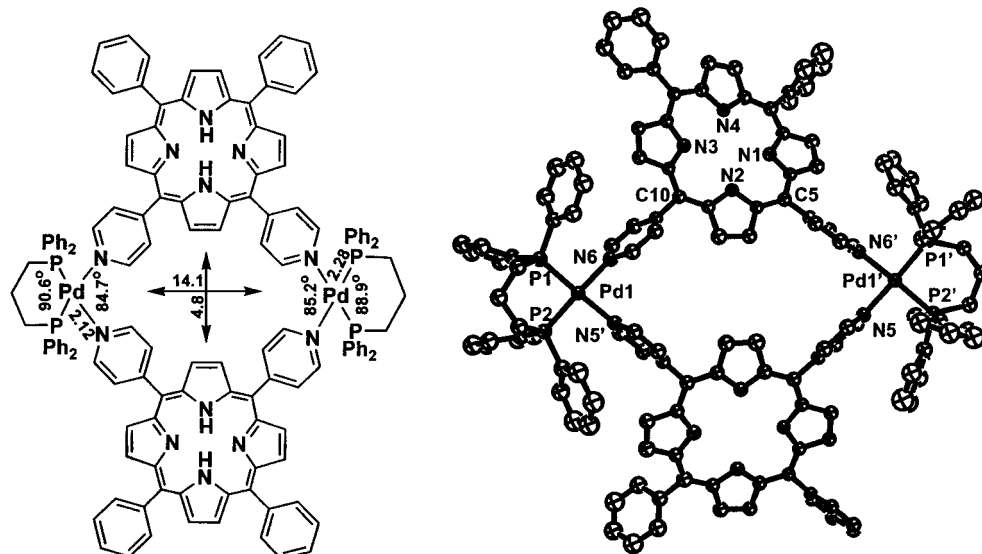


**Figure 5.** ORTEP plot representation and summary of important bond lengths and bond angles of the cationic portion of complex **8**.

to 6.7 Å and the effective C(quat)–C(quat) distance to 6.1 Å.

Especially interesting and revealing is the stacking pattern of complex **7** in the solid state, as shown in Figure 3. The cationic rhomboids are stacked along the *b*-axis, resulting in long channels that have also been found for similar molecular rectangles and molecular squares.<sup>20–22</sup> The repeating unit distance between each stacked cationic rhomboid is 14.1 Å, which is larger than that for the hybrid iodonium–transition metal square<sup>21</sup> (9.5 Å) or the neutral-charged mixed transition metal square<sup>20</sup> (10.7 Å), but about the same size as for Hupp's neutral rhenium square<sup>22</sup> (14.2 Å) or for the butterfly-like all transition metal 4,4'-bipyridine square (15.9 Å).<sup>23</sup> Both triflate counterions are disordered and were modeled by refining them in two positions, each with 50% occupancy. They are located within the channels above and below the rhomboidal planes, showing Pt–O interactions of 4.01 and 4.14 Å, respectively.

In addition to rhomboids **6a** and **7**, X-ray structure analysis of the 5,10-dipyridyl-15,20-dibenzylporphyrin-containing dinuclear palladium complex **8**<sup>19</sup> revealed a similar rhomboid-type structure (Figure 5).

For the Pd(II) centers of the 1,3-bis(diphenylphosphino)propane palladium corners of **8**, a square planar geometry with significant but characteristic deviations from the ideal 90° angles is found. While the average P–Pd–P angle is 89.7°, the average corresponding N–Pd–N angle is only 84.8°. The Pd–P and Pd–N bond lengths are normal and comparable to those in other macrocyclic systems.<sup>20,21</sup> To accommodate the smaller N–Pd–N angle and as a result of the inflexibility and rigidity of the cis-porphyrin system toward bending, the molecule adopts a butterfly-like geometry, with a dihedral angle between the two porphyrin rings of 164°. Due to favorable  $\pi$ – $\pi$  stacking interactions of the pyridyl rings with the phenyl rings of dppp, the two dpppPd corners are unsymmetrical, resulting in an E-configuration in the solid state. Moreover, steric repulsion between the dppp phenyl rings and the olefinic porphyrin protons causes additional twisting of the porphyrin ligands, resulting in an overall C<sub>1</sub> symmetric complex. The diagonal Pd–Pd distance is 14.1 Å, and the average distance between the two porphyrin rings is 4.8 Å, leaving almost no space for possible guest molecules (Figure 6).

The four triflate anions in **8** are located in sets of two above and below the square planar palladium, showing Pd–O distances of 3.83, 3.10, 3.66, and 3.86 Å. Seven molecules of ethanol and four molecules of water are

(22) Slone, R. V.; Hupp, J. T.; Stern, C. L.; Albrecht-Schmitt, T. E. *Inorg. Chem.* **1996**, *35*, 4096.

(23) Stang, P. J.; Cao, D. H.; Saito, S.; Arif, A. M. *J. Am. Chem. Soc.* **1995**, *117*, 6273.

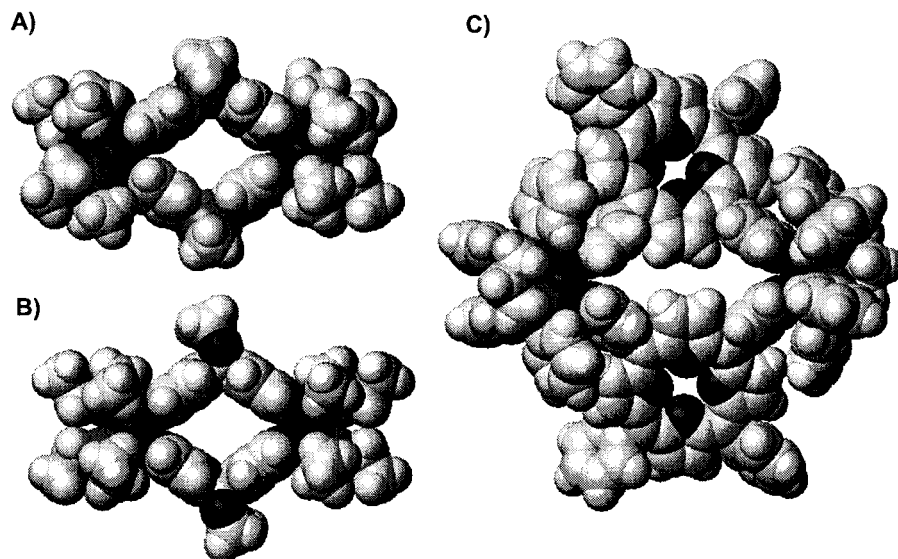


**Figure 6.** Space-filling models of **6a** (A), **7** (B), and **8** (C) based on X-ray data.

assigned per independent molecule located at no specific position between the self-assembled systems. Probably due to the butterfly-type of distortion and the large number of solvent molecules, no stacking of the porphyrin complexes is observed.

Finally, it is interesting to compare the geometry of **6a**, **7**, and **8** to the analogous dinuclear palladium macrocycles described by Fujita<sup>9</sup> as well as to the related dinuclear cyclophane reported by Diederich.<sup>10</sup>

For Diederich's fullerene-containing supramolecular assembly, values similar to **6a**, **7**, and **8** for the P–Pt–P (97.2°), N–Pt–N (81.6°), and C(py)–C(quat)–C(py) (113°) angles were found. While the inner N–Pt–N angle is almost identical, the tetrahedral bridgehead angle is widened. As a result, the sum of the inner angles (389°) is larger than in **6a** (381°) or **7** (384°), putting more strain on the system. In the case of Fujita's water-soluble ethylenediamine palladium system, the observed angles are slightly different. Although the angle in this complex at the quaternary carbon atom (107.0°) is similar to the ones in **6a** and **7**, the N(py)–Pd–N(py) bite angle is 89.6°. Thus, the sum of the inner angles in Fujita's ethylenediamine palladium system is even larger than in **6a**, in **7**, or in the fullerene system. As a consequence of this inflexibility, probably caused by the chelating ethylenediamine ligand, the pyridyl rings are bent toward the center of the cyclophane.

From these X-ray structures, the question of the limit to this type of self-assembly reaction, as a consequence of the observed ring strain, arose. To assemble a macrocycle with a higher strain energy, reaction of the 120° linker bis(4-pyridyl)ketone (**3**) with platinum bis-triflate complex **5a** was carried out in acetone. Surprisingly, analysis of the reaction mixture revealed the formation of one major product along with several minor products (<sup>1</sup>H and <sup>31</sup>P NMR).<sup>24</sup> Upon concentration and warming of the solution, the yield of the major product increased, suggesting the existence of a larger assembly rather than a dinuclear complex. Therefore, along with the quite different proton resonances observed for this compound (e.g., the resonance for the α-pyridyl protons is dramatically downfield shifted by Δδ ~ 0.6 ppm compared to all other dinuclear complexes), we assigned

this product to a trinuclear cyclic complex **9**. A similar tricyclic complex was also described by Che,<sup>25</sup> using sodium benzimidazol and a cis-Pt(II) complex as building units. Crystallization of **9** from aqueous acetone over two weeks gave colorless crystals of **10** as the only product in high yield. This product was assigned by its spectroscopic properties to one of the minor products observed in the reaction mixture.

X-ray structure analysis of **10** revealed a dinuclear macrocyclic rhomboid similar to the structures of **6a** and **7**, with the ketone function hydrated.<sup>26</sup> The reorganization of the self-assembled product occurred as a result of hydration of the bis(pyridyl)ketone and subsequent decrease of the dihedral angle at the hydrate carbon. Formation of an analogous hydrate product in water has already been described by Fujita.<sup>9</sup> Even though self-assembly of a less strained cyclotrimeric structure is favored under thermodynamic conditions, it seems that entropy effects play an important role in the self-assembly process of these macrocyclic systems, as pointed out by Raymond.<sup>1d</sup> Thus, the reduction of the angle around the carbonyl carbon atom from 120° (sp<sup>2</sup>) to approximately 109° (sp<sup>3</sup>) by forming the thermodynamically unfavorable hydrate appears to be a small price the system has to pay in order to form the smallest closed structure possible.<sup>9</sup>

## Conclusion

Cationic dinuclear rhomboids have been isolated via modular self-assembly of silicon- and carbon-based tectons with *cis* square planar platinum and palladium

(24) NMR data (acetone-*d*<sub>6</sub>) of the crude products in the reaction mixture of **3** with **5a**. <sup>1</sup>H NMR: major component **9**: δ = 9.43 (d, *J* = 6.0 Hz, α-pyridyl-H), 7.91 (d, *J* = 5.9 Hz, β-pyridyl-H), 2.11–1.87 (m, PCH<sub>2</sub>), 1.45–1.21 (m, CH<sub>2</sub>CH<sub>3</sub>); minor components: δ = 9.26 (d, α-pyridyl-H), 8.98 (d, *J* = 5.7 Hz, α-pyridyl-H), 8.84 (m, α-pyridyl-H), 8.02 (d, *J* = 5.7 Hz, β-pyridyl-H), 7.88 (d, *J* = 5.7 Hz, β-pyridyl-H), 7.70 (d, β-pyridyl-H), 7.59 (d, β-pyridyl-H), 2.11–1.87 (m, PCH<sub>2</sub>), 1.45–1.21 (m, CH<sub>2</sub>CH<sub>3</sub>). <sup>31</sup>P{<sup>1</sup>H} NMR: major component **9**: δ = 1.2 (s, <sup>1</sup>*J*(Pt,P) = 3061 Hz); minor components: δ = 2.0, 1.7, 1.0 (s, <sup>1</sup>*J*(Pt,P) = 3049 Hz).

(25) Lai, S.-W.; Chan, M. C.-W.; Peng, S.-M.; Che, C.-M. *Angew. Chem., Int. Ed.* **1999**, *38*, 669.

(26) Details on the X-ray structure analysis of complex **10** are available from the Supporting Information.

bistriflate complexes. The versatility of the coordination paradigm was shown by the use of diverse angular linkers to form similar rhomboid-like systems. In attempting to form a more strained system with larger bite angles, carbonyl hydration occurred to reduce the ring strain. In addition, we were able to show that entropy plays an important role in the formation of these macrocyclic systems, favoring the formation of the smallest cycle even though the hydration is thermodynamically disfavored. X-ray crystal structure analysis established molecules **6a** and **7** as planar rhomboids with small internal cavities of approximately  $10 \text{ \AA} \times 8 \text{ \AA}$ , whereas for the dinuclear porphyrin complex **8** a butterfly-type structure was observed. The stacking diagrams of **6a** and **7** have channel-like structures in the solid state that are likely to be important and useful for molecular host-guest interactions.

### Experimental Section

**General Comments.** The  $^1\text{H}$  NMR spectra were recorded at 300 MHz, and chemical shifts are reported relative to internal TMS  $\delta$  0.0 ppm or to the signal of a residual protonated solvent:  $\text{CDCl}_3$   $\delta$  7.27, acetone- $d_6$   $\delta$  2.05, or  $\text{CD}_3\text{CN}$   $\delta$  1.94 ppm. The  $^{13}\text{C}\{^1\text{H}\}$  NMR spectra were recorded at 75 MHz, and chemical shifts are reported relative to  $\text{CD}_3\text{CN}$   $\delta$  1.3 or  $\text{CDCl}_3$   $\delta$  77.2 ppm. The  $^{29}\text{Si}$  NMR spectra were recorded at 59.6 MHz, and chemical shifts are reported relative to external TMS  $\delta$  0.0 ppm. The  $^{31}\text{P}\{^1\text{H}\}$  NMR spectra were recorded at 121 MHz, and chemical shifts are reported relative to external 85% aqueous  $\text{H}_3\text{PO}_4$   $\delta$  0.0 ppm. The signals in the  $^1\text{H}$  NMR due to water are omitted. Elemental analyses were performed by Atlantic Microlab Inc., Norcross, GA. Melting points were obtained with a Mel-Temp capillary melting point apparatus and were not corrected. Mass spectra were obtained with a Finnigan MAT 95 mass spectrometer with a Finnigan MAT ICIS II operating system at 80 eV (EI), or under positive fast atom bombardment (FAB) conditions at 20 keV. 3-Nitrobenzyl alcohol was used as a matrix in  $\text{CH}_2\text{Cl}_2$  as a solvent, and polypropylene glycol and cesium iodide were used as a reference for peak matching. Electrospray mass spectra were obtained with a Micromass Quattro II with ionization performed under electrospray conditions (flow rate  $7.7 \mu\text{L}/\text{min}$ , capillary voltage 3.0 kV, cone 27 V, extractor 12 V). About 15 individual scans were averaged for the mass spectrum. The calibration of the mass range 100–3000 amu was done with a 1:1 mixture of an 2-propanol/water solution of NaI ( $2 \mu\text{g}/\mu\text{L}$ ) and CsI ( $0.01 \mu\text{g}/\mu\text{L}$ ). Samples were prepared as  $10 \text{ pg}/\mu\text{L}$  solutions in acetone just prior to the analysis.

**Materials.** Commercial reagents, 4-bromopyridine hydrochloride, dimethylsilicon dichloride, and diphenylsilicon dichloride, were ACS reagent grade or higher and were used without further purification. Methylene chloride was purified according to literature procedure<sup>27</sup> and distilled over  $\text{CaH}_2$ . Diethyl ether was purified according to literature procedure<sup>27</sup> and distilled over Na/benzophenone. Acetonitrile and chloroform used for spectroscopic measurements were spectrophotometric grade. Metal complexes **5a,b**<sup>28</sup> and di(4-pyridyl)ketone (**3**)<sup>29</sup> were prepared according to literature methods.

**Synthesis of Bis(4-pyridyl)silanes 2.** To a solution of 4-bromopyridine (**1**)<sup>30</sup> (7 mmol) in dry diethyl ether (20 mL)

under nitrogen was added dropwise *n*-butyllithium (7.2 mmol, 2.5 M solution in hexane) at  $-90^\circ\text{C}$ . The resulting mixture was allowed to warm to  $-30^\circ\text{C}$  and stirred at this temperature for 20 min. The yellow suspension was then cooled to  $-90^\circ\text{C}$ , and dichlorosilane (2.91 mmol) was added dropwise. Then the reaction mixture was slowly allowed to warm to room temperature, 6 N hydrochloric acid (10 mL) was added, and the diethyl ether solution was separated from the aqueous layer. The resulting organic solution was washed with 6 N hydrochloric acid ( $3 \times 10 \text{ mL}$ ). The combined aqueous solutions were stirred with decolorizing carbon for 1 h at room temperature. To the resulting solution was added saturated potassium hydroxide solution until its pH value was basic. Chloroform (50 mL) was added, and the aqueous layer was separated from the chloroform solution. The aqueous solution was washed with chloroform ( $2 \times 50 \text{ mL}$ ), and the combined organic layers were dried over  $\text{MgSO}_4$ . After evaporation of the solvent, the bis(4-pyridyl)silanes **2** were purified either by distillation ( $120^\circ\text{C}$ ,  $10^{-2}$  mbar) followed by column chromatography on silica gel with diethyl ether (**2a**, 24% yield) or by crystallization from diethyl ether (**2b**, 46% yield).

**(Dimethyl)bis(4-pyridyl)silane (2a):** yellow oil; 24%; bp  $120^\circ\text{C}$ ,  $10^{-2}$  mbar;  $^1\text{H}$  NMR ( $\text{CDCl}_3$ )  $\delta$  = 8.45 (dd,  $J$  = 5.2 Hz,  $J$  = 1.7 Hz, 4 H,  $\alpha$ -pyridyl-H), 7.23 (dd,  $J$  = 5.3 Hz,  $J$  = 1.7 Hz, 4 H,  $\beta$ -pyridyl-H), 0.47 (s, 6 H, Me);  $^{13}\text{C}\{^1\text{H}\}$  NMR ( $\text{CDCl}_3$ )  $\delta$  = 148.6 (s,  $\alpha$ -pyridyl-C), 145.8 (s, ipso-pyridyl-C), 128.2 (s,  $\beta$ -pyridyl-C), -4.1 (s, Me);  $^{29}\text{Si}$  NMR ( $\text{CD}_3\text{CN}$ )  $\delta$  = -0.7 (s); EI-MS (80 eV)  $m/z$  (%) 214.1 (70) [ $\text{M}^+$ ], 199.0 (100) [ $\text{M}^+$  - Me], 136.0 (31) [ $\text{M}^+$  - pyridine].

**(Diphenyl)bis(4-pyridyl)silane (2b):** white solid; 46%; mp  $218^\circ\text{C}$ ;  $^1\text{H}$  NMR ( $\text{CDCl}_3$ )  $\delta$  = 8.64 (dd,  $J$  = 5.3 Hz,  $J$  = 1.8 Hz, 4 H,  $\alpha$ -pyridyl-H), 7.54–7.41 (unresolved m, 14 H, Ar-H +  $\beta$ -pyridyl-H);  $^{13}\text{C}\{^1\text{H}\}$  NMR ( $\text{CDCl}_3$ )  $\delta$  = 149.3 (s,  $\alpha$ -pyridyl-C), 143.1 (s, ipso-pyridyl-C), 136.4 (s,  $\beta$ -pyridyl-C), 130.88 (s, ipso-Ph-C), 130.84 (s, para-Ph-C), 130.78 (s, ortho-Ph-C), 128.6 (s, meta-Ph-C);  $^{29}\text{Si}$  NMR ( $\text{CDCl}_3$ )  $\delta$  = -10 (s); EI-MS (80 eV)  $m/z$  (%) 338.1 (96) [ $\text{M}^+$ ], 260.0 (100) [ $\text{M}^+$  - pyridine];  $\text{C}_{22}\text{H}_{18}\text{N}_2\text{Si}\cdot\text{H}_2\text{O}$  (356.5) calcd C 74.12, H 5.65, N 7.68; found C 74.66, H 5.25, N 7.77.

**2,2-Bis(4-pyridyl)-1,3-dioxolane (4).** Di(4-pyridyl)ketone (**3**) (102.8 mg, 0.56 mmol) was dissolved in toluene (8 mL). 2-Bromoethanol (0.19 mL, 2.73 mmol) was then added by syringe. Within moments a white precipitate formed and dropped out of solution. DBU, 1,8-diazabicyclo-[5,4,0]-undec-7-ene (0.29 mL, 1.95 mmol), was syringed into the reaction, upon which the precipitate redissolved. The reaction was allowed to stir overnight, and once again a white precipitate formed. The reaction mixture was washed through a plug of silica gel with acetone, then the solvent was removed in vacuo. The product was then redissolved in chloroform and precipitated with hexane, dried in vacuo, and used as is (92.0 mg, 72%): mp  $136^\circ\text{C}$ ; IR (thin film)  $\text{cm}^{-1}$  = 2990, 2899 (aromatic C-H stretch), 1595 (aromatic ring stretch), 1222 (asym C-O-C stretch);  $^1\text{H}$  NMR ( $\text{CD}_3\text{NO}_2$ )  $\delta$  = 8.55 (d,  $J$  = 6.1 Hz, 4 H,  $\alpha$ -pyridyl-H), 7.46 (d,  $J$  = 6.1 Hz, 4 H,  $\beta$ -pyridyl-H), 4.11 (s, 4 H,  $\text{CH}_2$ );  $^{13}\text{C}\{^1\text{H}\}$  NMR ( $\text{CD}_3\text{NO}_2$ )  $\delta$  = 151.3 (s,  $\alpha$ -pyridyl-C), 151.1 (s, ipso-pyridyl-C), 121.9 (s,  $\beta$ -pyridyl-C), 108.3 (s, O-C-O), 66.7 (s,  $\text{CH}_2$ ); EI-MS (80 eV)  $m/z$  (%) 228.1 (0.1) [ $\text{M}^+$ ], 150.0 (100) [ $\text{M}^+$  - pyridine];  $\text{C}_{13}\text{H}_{12}\text{N}_2\text{O}_2$  (228.3) calcd C 68.41, H 5.3, N 12.27; found C 68.30, H 5.35, N 12.19.

**Synthesis of Rhomboids 6.** To a solution of metal bistriflate complex **5** (0.04 mmol) in acetone (5 mL) was added (bispyridyl)silane **2** (0.04 mmol). After stirring the reaction mixture for 30 min at  $20^\circ\text{C}$  the solvent was removed in vacuo and compounds **6** were isolated as solids in essentially quantitative yield.

**Cyclobis[*cis*-Pt-bis(triethylphosphine)][dimethylbis(4-pyridyl)silane] $^{2+}$ (-OSO<sub>2</sub>CF<sub>3</sub>)<sub>2</sub> (6a):** white solid; 99%; mp  $273\text{--}278^\circ\text{C}$  (dec);  $^1\text{H}$  NMR ( $\text{CD}_3\text{CN}$ )  $\delta$  = 8.42 (d,  $J$  = 5.7 Hz, 8 H,  $\alpha$ -pyridyl-H), 7.47 (d,  $J$  = 5.7 Hz, 8 H,  $\beta$ -pyridyl-H), 1.60 (pp, 24 H,  $\text{CH}_2$ ), 0.97 (dt,  $^3J(\text{P,H})$  = 18.0 Hz,  $^3J(\text{H,H})$  = 7.2

(27) Perrin, D. D.; Armarego, W. L. F. *Purification of Laboratory Chemicals*; Pergamon: Oxford, 1988.

(28) Stang, P. J.; Cao, D. H.; Saito, S.; Arif, A. M. *J. Am. Chem. Soc.* **1995**, *117*, 6273.

(29) (a) Minn, F. L.; Trichilo, C. L.; Hurt, C. R.; Filipescu, N. *J. Am. Chem. Soc.* **1970**, *92*, 3600. (b) See ref 9.

(30) 4-Bromopyridine hydrochloride was deprotected with NaOH in  $\text{Et}_2\text{O}/\text{H}_2\text{O}$ , the resulting 4-bromopyridine solution was dried over  $\text{MgSO}_4$  and  $\text{CaH}_2$  and stored under nitrogen and exclusion of light.

Hz, 36 H, CH<sub>2</sub>CH<sub>3</sub>), 0.42 (s, 12 H, SiCH<sub>3</sub>); <sup>13</sup>C{<sup>1</sup>H} NMR (CD<sub>3</sub>CN) δ = 154.6 (s, ipso-pyridyl-C), 149.9 (s, α-pyridyl-C), 133.5 (s, β-pyridyl-C), 15.4 (m, CH<sub>2</sub>), 8.2 (s, CH<sub>2</sub>CH<sub>3</sub>), -5.8 (s, SiCH<sub>3</sub>); <sup>31</sup>P{<sup>1</sup>H} NMR (CD<sub>3</sub>CN) δ = 4 (s, <sup>1</sup>J(Pt,P) = 3073 Hz); <sup>29</sup>Si NMR (CD<sub>3</sub>CN) δ = 0.6 (s); MS (FAB) *m/z* 1738 [M<sup>+</sup> - OTf] calcd 1738; MS (ES) *m/z* 1738 [M<sup>+</sup> - OTf] calcd 1738; C<sub>52</sub>H<sub>88</sub>F<sub>12</sub>N<sub>4</sub>O<sub>12</sub>P<sub>4</sub>Pt<sub>2</sub>S<sub>4</sub>Si<sub>2</sub>·2H<sub>2</sub>O (1923.8) calcd C 32.47, H 4.82, N 2.91, S 6.67; found C 32.19, H 4.75, N 2.79, S 6.35.

**Cyclobis[*cis*-Pt-bis(triethylphosphine)][diphenylbis-(4-pyridyl)silane]<sup>2+</sup>(-OSO<sub>2</sub>CF<sub>3</sub>)<sub>2</sub>] (6b):** white solid; 98%; mp 302–308 °C (dec); <sup>1</sup>H NMR (CD<sub>3</sub>CN) δ = 8.66 (d, *J* = 6.0 Hz, 8 H, α-pyridyl-H), 7.73 (d, *J* = 6.0 Hz, 8 H, β-pyridyl-H), 7.68–7.48 (m, 20 H, phenyl-H), 1.81 (pq, 24 H, CH<sub>2</sub>), 1.21 (dt, <sup>3</sup>J(P,H) = 18.0 Hz, <sup>3</sup>J(H,H) = 7.5 Hz, 36 H, CH<sub>2</sub>CH<sub>3</sub>); <sup>13</sup>C{<sup>1</sup>H} NMR (CD<sub>3</sub>CN) δ = 150.5 (s, ipso-pyridyl-C), 150.3 (s, α-pyridyl-C), 137.4 (s, β-pyridyl-C), 135.2, 132.8, 130.1 (each s, *o*-, *m*-, *p*-phenyl-C), 128.5 (s, ipso-phenyl-C), 15.7 (m, CH<sub>2</sub>), 8.3 (s, CH<sub>2</sub>CH<sub>3</sub>); <sup>31</sup>P{<sup>1</sup>H} NMR (CD<sub>3</sub>CN) δ = 5 (s, <sup>1</sup>J(Pt,P) = 3071 Hz); <sup>29</sup>Si NMR (CD<sub>3</sub>CN) δ = -11 (s); MS (FAB) *m/z* 1987 [M<sup>+</sup> - OTf] calcd 1988; MS (ES) *m/z* 918 [(M/2)<sup>+</sup> - OTf] calcd 918; C<sub>72</sub>H<sub>96</sub>F<sub>12</sub>N<sub>4</sub>O<sub>12</sub>P<sub>4</sub>Pt<sub>2</sub>S<sub>4</sub>Si<sub>2</sub> (2134.4) calcd C 40.49, H 4.53, N 2.62, S 6.00; found C 40.04, H 4.57, N 2.59, S 5.81.

**Cyclobis[*cis*-Pd-bis(triethylphosphine)][dimethylbis-(4-pyridyl)silane]<sup>2+</sup>(-OSO<sub>2</sub>CF<sub>3</sub>)<sub>2</sub>] (6c):** yellow-white solid; 99%; mp 167–173 °C (dec); <sup>1</sup>H NMR (CD<sub>3</sub>CN) δ = 8.40 (d, *J* = 6.3 Hz, 8 H, α-pyridyl-H), 7.39 (d, *J* = 6.6 Hz, 8 H, β-pyridyl-H), 1.48 (pq, 24 H, CH<sub>2</sub>), 0.96 (dt, <sup>3</sup>J(P,H) = 18.0 Hz, <sup>3</sup>J(H,H) = 7.2 Hz, 36 H, CH<sub>2</sub>CH<sub>3</sub>), 0.44 (s, 12 H, SiCH<sub>3</sub>); <sup>13</sup>C{<sup>1</sup>H} NMR (CD<sub>3</sub>CN) δ = 153.6 (s, ipso-pyridyl-C), 149.8 (s, α-pyridyl-C), 132.8 (s, β-pyridyl-C), 16.6 (m, CH<sub>2</sub>), 8.5 (s, CH<sub>2</sub>CH<sub>3</sub>), -5.6 (s, SiCH<sub>3</sub>); <sup>31</sup>P{<sup>1</sup>H} NMR (CD<sub>3</sub>CN) δ = 32 (s); <sup>29</sup>Si NMR (CD<sub>3</sub>CN) δ = 0.4 (s); MS (ES) *m/z* 1560 [M<sup>+</sup> - OTf] calcd 1559.

**Cyclobis[*cis*-Pd-bis(triethylphosphine)][diphenylbis-(4-pyridyl)silane]<sup>2+</sup>(-OSO<sub>2</sub>CF<sub>3</sub>)<sub>2</sub>] (6d):** yellow-white solid; 98%; mp 219–222 °C (dec); <sup>1</sup>H NMR (CD<sub>3</sub>CN) δ = 8.70 (d, *J* = 5.7 Hz, 8 H, α-pyridyl-H), 7.66–7.41 (m, 28 H, β-pyridyl- and phenyl-H), 1.87 (pq, 24 H, CH<sub>2</sub>), 1.25 (dt, <sup>3</sup>J(P,H) = 18.0 Hz, <sup>3</sup>J(H,H) = 7.5 Hz, 36 H, CH<sub>2</sub>CH<sub>3</sub>); <sup>13</sup>C{<sup>1</sup>H} NMR (CD<sub>3</sub>CN) δ = 150.4 (s, β-pyridyl-C), 148.8 (s, ipso-pyridyl-C), 137.3 (s, β-pyridyl-C), 134.3, 132.6, 129.9 (each s, *o*-, *m*-, *p*-phenyl-C), 129.2 (s, ipso-phenyl-C), 17.0 (m, CH<sub>2</sub>), 8.6 (s, CH<sub>2</sub>CH<sub>3</sub>); <sup>31</sup>P{<sup>1</sup>H} NMR (CD<sub>3</sub>CN) δ = 36 (s); <sup>29</sup>Si NMR (CD<sub>3</sub>CN) δ = -10 (s); MS (FAB): *m/z* 1809 [M<sup>+</sup> - OTf] calcd 1807; MS (ES) *m/z* 829 [(M/2)<sup>+</sup> - OTf] calcd 829.

**Cyclobis[*cis*-Pt-bis(triethylphosphine)][2,2-bis(4-pyridyl)-1,3-dioxolane]<sup>2+</sup>(-OSO<sub>2</sub>CF<sub>3</sub>)<sub>2</sub>] (7):** To a solution of platinum complex **5a** (0.04 mmol) in CD<sub>3</sub>CN (3 mL) was added di(4-pyridyl)acetal (**4**) (0.04 mmol). After 30 min the solvent was removed in vacuo and product **7** was obtained as a solid: 97% yield; mp 214–218 °C (dec); <sup>1</sup>H NMR (CD<sub>3</sub>CN) δ = 8.83 (d, *J* = 5.1 Hz, 8 H, α-pyridyl-H), 7.70 (d, *J* = 6.3 Hz, 8 H, β-pyridyl-H), 4.04 (s, 8 H, OCH<sub>2</sub>), 1.73 (pq, 24 H, PCH<sub>2</sub>), 1.20 (dt, <sup>3</sup>J(P,H) = 17.7 Hz, <sup>3</sup>J(H,H) = 7.5 Hz, 36 H, CH<sub>2</sub>CH<sub>3</sub>); <sup>13</sup>C{<sup>1</sup>H} NMR (CD<sub>3</sub>CN) δ = 154.1 (s, ipso-pyridyl-C), 151.4 (s, α-pyridyl-C), 125.0 (s, β-pyridyl-C), 105.3 (O–C–O), 66.5 (OCH<sub>2</sub>), 15.3 (m, PCH<sub>2</sub>), 7.9 (s, CH<sub>2</sub>CH<sub>3</sub>); <sup>31</sup>P{<sup>1</sup>H} NMR (CD<sub>3</sub>CN) δ = 0.2 (s, <sup>1</sup>J(Pt,P) = 3079 Hz); MS (ES) *m/z* 808 [(M/2)<sup>+</sup> - OTf] calcd 808; C<sub>54</sub>H<sub>84</sub>F<sub>12</sub>N<sub>4</sub>O<sub>16</sub>P<sub>4</sub>Pt<sub>2</sub>S<sub>4</sub> (1914.3) calcd C 33.86, H 4.42, N 2.92, S 6.69; found C 34.16, H 4.69, N 2.84, S 6.27.

**[Pd(dppp)(*cis*-DpyDpp)][OSO<sub>2</sub>CF<sub>3</sub>]<sub>4</sub> (8):** Complex **8** was prepared according to a literature procedure.<sup>19</sup>

**Cyclobis[*cis*-Pt-bis(triethylphosphine)][dihydroxybis-(4-pyridyl)methane]<sup>2+</sup>(-OSO<sub>2</sub>CF<sub>3</sub>)<sub>2</sub>] (10):** To a solution of

platinum complex **5a** (0.1 mmol) in acetone (3 mL) was added di(4-pyridyl)ketone (**3**) (0.1 mmol). NMR control of the reaction mixture revealed several products.<sup>24</sup> Over a period of 14 days in aqueous acetone compound **10** was isolated as colorless crystals: 95% yield; <sup>1</sup>H NMR (acetone-*d*<sub>6</sub>) δ = 8.98 (d, *J* = 5.7 Hz, 8H, α-pyridyl-H), 7.88 (d, *J* = 5.7 Hz, 8H, β-pyridyl-H), 2.11–1.87 (m, 24H, PCH<sub>2</sub>), 1.45–1.21 (m, 36H, CH<sub>2</sub>CH<sub>3</sub>); <sup>31</sup>P{<sup>1</sup>H} NMR (acetone-*d*<sub>6</sub>): δ = 1.0 (s, <sup>1</sup>J(Pt,P) = 3049 Hz); C<sub>50</sub>H<sub>80</sub>F<sub>12</sub>N<sub>4</sub>O<sub>16</sub>P<sub>4</sub>Pt<sub>2</sub>S<sub>4</sub> (1767.3) calcd C 32.23, H 4.33, N 3.01, S 6.88; found C 32.45, H 4.21, N 3.14, S 6.76.

**X-ray Crystal Structure Determination.** Single crystals suitable for X-ray crystallography were grown by evaporation of an acetone solution of **6a** and **7** at ambient temperature. Crystals of **8** were grown from a chloroform solution. The crystals were mounted on a glass fiber with tiny traces of viscous oil and then transferred to a Nonius Kappa CCD diffractometer equipped with Mo Kα radiation (λ = 0.71073 Å). Ten frames of data were collected at 200(0.1) K with an oscillation range of 1 deg/frame and an exposure time of 20 s/frame.<sup>31</sup> Indexing and unit cell refinement based on all observed reflection from those 10 frames indicated a monoclinic P lattice. The reflections were indexed, integrated, and corrected for Lorentz, polarization, and absorption effects using DENZO-SMN and SCALEPAC.<sup>32</sup> Axial photographs and systematic absences were consistent with the compound having crystallized in the appropriate space groups.

The structures were solved by a combination of direct methods and heavy atom using SIR 97.<sup>33</sup> All of the non-hydrogen atoms were refined with anisotropic displacement coefficients *U*(H) = 1.2*U*(C) or 1.5*U*(Cmethyl), and their coordinates were allowed to ride on their respective carbons using SHELXL97.<sup>34</sup> The weighting scheme employed was *w* = 1/[σ<sup>2</sup>(*F*<sub>o</sub><sup>2</sup>) + (0.0194*P*)<sup>2</sup> + 14.26*P*] for **6a**, *w* = 1/[σ<sup>2</sup>(*F*<sub>o</sub><sup>2</sup>) + (0.0247*P*)<sup>2</sup> + 27.147*P*] for **7** and *w* = 1/[σ<sup>2</sup>(*F*<sub>o</sub><sup>2</sup>) + (0.1512*P*)<sup>2</sup> + 14.940*P*] for **8** where *P* = (*F*<sub>o</sub><sup>2</sup> + 2*F*<sub>c</sub><sup>2</sup>)/3.<sup>35</sup>

**Acknowledgment.** We thank the National Science Foundation (CHE-9818472) and the National Institutes of Health (5R01GM57052) for support, and the Alexander von Humboldt Foundation for a Feodor Lynen Fellowship to M.S. and S.L., respectively.

**Supporting Information Available:** Crystal structure data for **6a**, **7**, **8**, and **10** including tables of calculated positional parameters and *U* for the hydrogen atoms, non-hydrogen positional parameters and anisotropic thermal parameters, and complete bond lengths, angles, and torsional angles are provided. This material is available free of charge via the Internet at <http://pubs.acs.org>.

OM990567S

(31) COLLECT Data Collection Software; Nonius B. V., 1998.

(32) Otwinowski, Z.; Minor, W. Processing of X-ray Diffraction Data Collected in Oscillation Mode. *Methods Enzymol.* **1997**, *276*, 307–326.

(33) Altomare, A.; Burla, M. C.; Camalli, M.; Cascarano, G.; Giacovazzo, C.; Guagliardi, A.; Molteni, A. G. G.; Polidori, G.; Spagna, R. *SIR97* (Release 1.02)—A program for automatic solution and refinement of crystal structure.

(34) Sheldrick, G. M. *SHELXL97* [Includes *SHELXS97*, *SHELXL97*, *CIFTAB*]—Programs for Crystal Structure Analysis (Release 97–2); University of Göttingen: Germany, 1997.

(35) *R*<sub>1</sub> = Σ(|*F*<sub>o</sub> − |*F*<sub>c</sub>||) / Σ|*F*<sub>o</sub>|, *wR*<sub>2</sub> = [Σ(*w*(*F*<sub>o</sub><sup>2</sup> − *F*<sub>c</sub><sup>2</sup>)<sup>2</sup>) / Σ(*F*<sub>o</sub><sup>2</sup>)<sup>1/2</sup>]<sup>1/2</sup>, and *S* = goodness-of-fit on *F*<sup>2</sup> = [Σ(*w*(*F*<sub>o</sub><sup>2</sup> − *F*<sub>c</sub><sup>2</sup>)<sup>2</sup>) / (n − p)]<sup>1/2</sup>, where *n* is the number of reflections and *p* is the number of parameters refined.